Flow kinematics characteristics of extreme waves impacting on a vertical seawall

Chao Wang, Yuxiang Ma*

State Key Laboratory of Coastal and Ocean Engineering, Dalian University of Technology, Dalian, China
E-mail: yuxma@dlut.edu.cn

1 INTRODUCTION

Under the context of global climate change, the increasing frequency and intensity of extreme wave events pose significant challenges to coastal and ocean engineering structures [1,2]. Among these, the interaction of extreme waves with vertical seawalls often leads to violent slamming and overtopping, which involve complex hydrodynamic phenomena such as impulsive jet impact, intense turbulent diffusion, and multi-phase flow mixing. These processes not only induce high-impact loads on the structure but also convey substantial wave energy landward, potentially compromising the safety of protected area.

While existing research has largely focused on time-averaged overtopping discharges several key mechanistic aspects remain poorly understood. These include the instantaneous evolution of the flow after wave crest impact, the spatial distribution of impact energy, and the turbulence characteristics within the aerated landward flow [2]. The lack of a refined understanding of such multi-phase dynamics limits the accurate prediction of hydrodynamic loads under extreme wave conditions. To address this gap, the present study systematically investigates the flow kinematics and pressure characteristics associated with extreme wave slamming and overtopping on a vertical seawall.

2. METHODOLOGY

A high-fidelity two-phase numerical wave flume was established using the open-source CFD platform OpenFOAM to investigate the flow kinematics characteristics of extreme waves impacting on a vertical seawall [3]. The Reynolds-Averaged Navier-Stokes (RANS) equations were coupled with the Volume of Fluid (VOF) method to capture the flow motion and free surface deformation, while the waves2Foam toolbox was utilized for accurate wave generation and absorption. To ensure the reliability of the numerical simulations, corresponding physical model tests were conducted, with the experimental setup illustrated in Fig. 1.
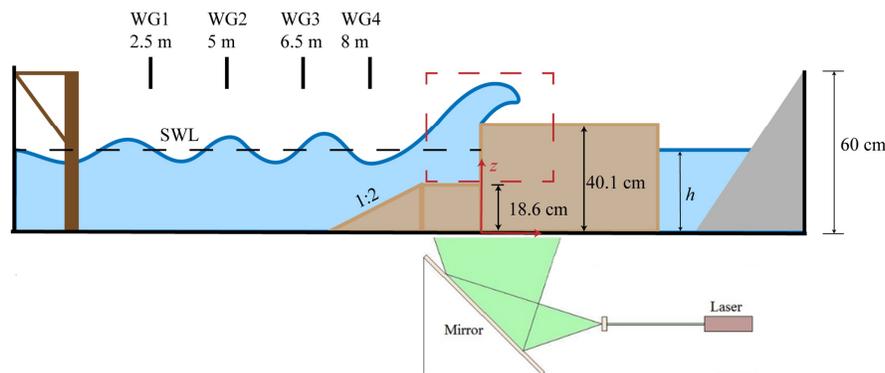

Fig. 1 Sketch of the experimental setup

A representative case with an incident wave amplitude of $A_f = 0.08$ m was selected for the initial validation. Fig. 2 compares the time series of free-surface elevation between the numerical predictions and experimental measurements at various gauge locations. The numerical results exhibit excellent agreement with the experimental data regarding both wave phase and crest elevation, confirming the model's capability to accurately replicate nonlinear wave propagation.
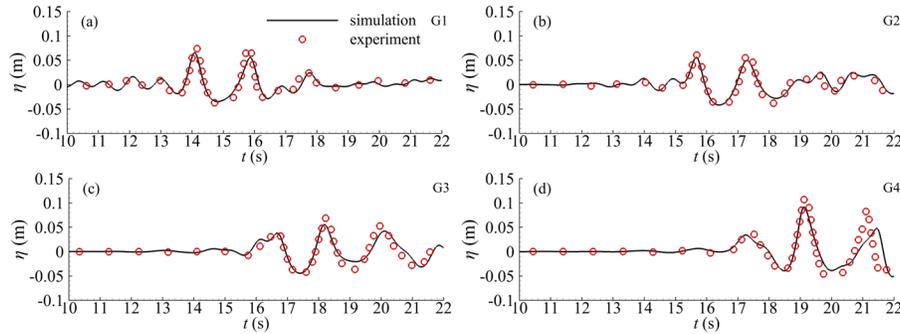

Fig. 2 Comparisons of time series of water surface elevation at different wave gauges

In this study, incident waves were generated based on the JONSWAP spectrum (f = 0.1 to 2.0 Hz) with a constant water depth of 0.316 m. A series of cases with incident wave amplitudes ranging from 0.06 m to 0.10 m were simulated to examine the hydrodynamic response under different intensities. The detailed wave parameters and structural settings are listed in Table 1.

Tab. 1 Table of experimental cases

Case	Water depth (m)	Frequency f (Hz)	Peak period T (s)	Spectral type	Focusing time (s)	Focusing position (m)	Wave amplitude A_f (m)
R1							0.060
R2							0.065
R3							0.070
R4							0.075
R5	0.316	0.1~2.0;	1.82	Jonswap	20	9.2	0.080
R6							0.085
R7							0.090
R8							0.095
R9							0.100

3 RESULTS AND DISCUSSION

In this study, the flow kinematics of wave slamming and overtopping were investigated by varying the incident wave amplitude to reveal the specific influence of wave height on the process. Due to space limitations, only the representative case with an incident wave amplitude of $A_f = 0.08$ m is presented here, where the numerical predictions are compared with snapshots captured from physical experiments (Fig. 3). Overall, the flow evolution exhibits qualitative similarities across different wave heights, following a consistent sequence: wave crest run-up (Fig. 8a), the formation

of an upward jet in front of the wall (Fig. 3b), the downfall of the overtopping water (Fig. 3c), and the subsequent backflow on the seawall top (Fig. 3d). However, distinct differences are observed in the flow morphology, particularly regarding the slamming mechanics on the seawall top. For smaller incident waves ($A_f = 0.08$ m), the vertical excursion of the upward jet is limited with a continuous free surface, and the flow exhibits minimal air entrainment, characterizing a quasi-single-phase overtopping state. Conversely, when the incident wave amplitude exceeds 0.08 m, the process transitions to a mixed regime of bulk water overtopping and an upper slamming jet. This state involves significant aeration and induces pronounced slamming phenomena on the seawall top (Fig. 3c).
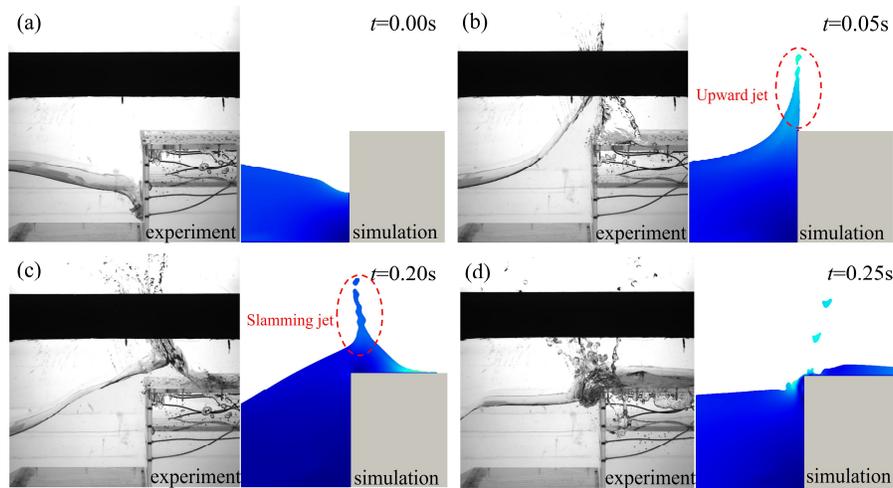

Fig. 3 Comparisons of flow evolution during the slamming process

Fig. 4 presents the velocity fields during the slamming process for the case with an incident wave amplitude of $A_f = 0.08$ m, where the numerical predictions are compared with the flow fields measured using PIV and BIV techniques in the experiments. Prior to the contact between the wave crest and the wall, no breaking occurs, and the overall flow velocity is directed towards the wave propagation direction (Fig. 4a). Upon contact, the vertical velocity at the impact point increases rapidly, and the wave run-up gradually evolves into an upward jet (Fig. 4b). The maximum velocity during this run-up process reaches 3.4 V_c/C_0, where C_0 denotes the celerity of the incident wave crest. As the run-up exceeds the seawall height, the water mass ejects over the top. Due to the shoreward velocity component of the lower water body, the loss of horizontal constraint from the vertical wall drives the crest water to overturn shoreward (Fig. 4c). After reaching its peak elevation, the overtopping flow enters the downfall phase. The falling water is primarily concentrated on the seawall top area, with the maximum downfall velocity occurring within the range of $0 \leq x \leq 0.10$ m, peaking at 2.8 V_c/C_0 (Fig. 4d). As the overtopping water moves shoreward, the flow velocity on the seawall top becomes dominated by the horizontal shoreward component, with a maximum velocity of approximately 1.2 V_c/C_0 (Fig. 4e). In addition, this study compares different types of overtopping flows, revealing the significant influence of incident wave height on the vertical velocity distribution on the seawall top. Furthermore, the distribution patterns of the Coefficient of Variation for peak pressures and flow velocities at the front section of the seawall top are presented.
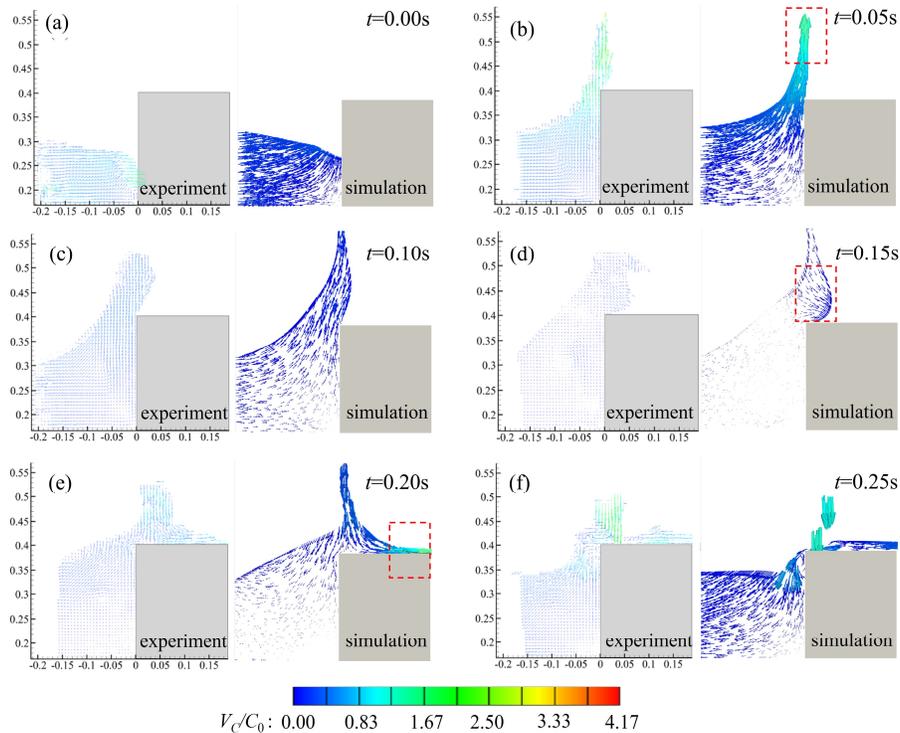
Fig. 4 Comparisons of velocity fields during the slamming process

4 CONCLUSIONS

This study investigated the flow kinematics characteristics of extreme waves impacting on a vertical seawall, focusing on the flow evolution during the overtopping process. The results indicate that the interaction involves four distinct flow stages: wave crest run-up in front of the wall, the formation of an upward jet, the downfall of the overtopping water, and the slamming flow on the seawall top. Additionally, in the slamming overtopping regime, which is characterized by violent air-water interaction, the run-up height, maximum vertical velocity, and peak pressure on the seawall top exhibit an exponential relationship with the incident wave height. Furthermore, the Coefficient of Variation (COV) of the flow velocity shows an overall positive correlation with that of the slamming pressure, with the instability of the peak pressure being notably higher than that of the flow velocity.

REFERENCES

[1] Ma, Y., Tai, B., Xie, B., Xu, T., Perlin, M., and Dong, G, 2023. Progress in the research of wave slamming forces on vertical cylinders. *Journal of Marine Science and Application*, *22*(1), 1-13.

[2] Tai, B., Ma, Y., Dong, G., Koh, C. G., Tang, T. , and Perlin, M, 2023. An enhanced model for an extreme wave impacting a vertical cylinder. *Coastal Engineering*, *194*, 104630.

[3] Steer, J. N., Kimmoun, O. , and Dias, F, 2021. Breaking-wave induced pressure and acceleration on a clifftop boulder. *Journal of Fluid Mechanics*, *929*, R1.

[4] Jasak, H. , 2009 . OpenFOAM: Open source CFD in research and industry. *International journal of naval architecture and ocean engineering*, *1*(2), 89-94.